PHYSICAL REVIEW A VOLUME 1, NUMBER 2 FEBRUARY 1970

Propagation of a Gaussian Light Pulse through an Anomalous Dispersion Medium

C. G. B. Garrett and D. E. McCumber

Bell Telephone Laboratories, Murray Hill, New Jersey 07981

(Received 25 September 1969)

The propagation of a Gaussian light pulse through a medium having a positive or negative absorption line is examined. Analytical approximations are obtained for the case where the spectral width of the pulse is much smaller than that of the line. It is shown that the pulse remains substantially Gaussian and unchanged in width for many exponential absorption depths, and that the locus of instants of maximum amplitude follows the classical expression for the group velocity, even if this is greater than the velocity of light, or negative. Numerical calculations have been used to examine what happens beyond the limit of usefulness of the analytical approximations.

I. INTRODUCTION

When an electromagnetic signal of frequency ν propagates through a nonabsorptive but dispersive medium, the phase velocity is c/n, where n is the refractive index, while the group velocity is $c/[n+\nu(dn/d\nu)]$. So long as $dn/d\nu > 0$, corresponding to "normal" dispersion, the group velocity is less than the phase velocity. When the medium has an absorption line near the optical frequency ν, the expression $c/[n+\nu(dn/d\nu)]$ can become larger than c, or even negative. Under these conditions, however, the role of the associated absorption is such as to destroy the elementary identification of the group velocity with the velocity at which the energy associated with some signal is propagated. Nevertheless, there exist conditions under which the expression $c/[n+\nu(dn/d\nu)]$ has a clear physical interpretation, even when the expression is negative.

It seems generally to be taken for granted that an incident signal pulse will necessarily be distorted to the extent that the idea of a group velocity loses its meaning. In a series of classic papers, Sommerfeld[1,2] and Brillouin[2,3] investigated the response of a semi-infinite anomalous dispersion medium to an incident sinusoidal signal whose amplitude was zero before some initial time t_0, and unity thereafter. This work showed that the main signal reaches a depth z at a time which is always greater than t_0+z/c; however, the main signal is preceded by "precursors," the front edges of which travel at c and at $c/\sqrt{\epsilon}$, where ϵ is the dc dielectric constant. These precursors correspond, respectively, to the Fourier components of limitlessly large and vanishingly small frequency, and have been observed experimentally.[4]

A situation more easily realizable in the laboratory is one in which the pulse has smoothly time-varying front and back edges. A Gaussian pulse has such a form and also is convenient for analytical work. The pulses occurring in some mode-locked lasers are very nearly Gaussian.

Suppose such a pulse passes through a slab of some linear but dispersive medium having an absorption line (positive or negative) in the vicinity of the central frequency of the pulse. What is the form of the pulse emerging from the slab, and when will it emerge? In this paper we tackle these questions. We assume throughout that the response of the medium is linear – that is, the dielectric function $n(\omega)$ is not modified by the presence or absence of the electromagnetic signal.

Our analysis is restricted to the case where the relative changes with frequency of n itself are small in comparison with unity, but this restriction does not mean that the changes in $c/[n+\nu(dn/d\nu)]$ are small in comparison with c, if the line is sufficiently narrow. We shall show that, provided the slab is not too thick, the power spectrum of the emerging pulse is still substantially Gaussian, and the peak of the pulse emerges at the instant given by the classical group velocity expression, *even if that instant is earlier than the instant at which the peak of the input pulse entered the slab*. For thicker slabs, the power spectrum is sufficiently distorted that the classical group velocity expression no longer applies. In this case our simple analytical approximations break down, and we have had to resort to numerical techniques. However, the relevance of these last techniques to experimental conditions that can actually be achieved in the laboratory is rather small, since, so long as the pulse is spectrally narrow in comparison with the atomic line, significant distortion will generally not occur until the over-all gain or attenuation is enormously large.

II. GENERAL FORMULATION OF THE PROBLEM

We restrict our attention to a plane-wavefront electromagnetic field,

$$\vec{E}(\vec{r},t)=\vec{E}_0 f(z,t) \quad , \tag{1}$$

propagating in the positive z direction in a linear but dispersive medium which fills the half-plane $z>0$. Because the medium is dispersive, $f(z,t)$ is not simply a function of $z-\bar{c}t$ with $\bar{c}$ some constant velocity.

We assume for each $z \geq 0$ that the function $f(z,t)$ is limited temporally in the sense that the Fourier transform

$$\tilde{f}(z,\omega)=\int_{-\infty}^{\infty} dt e^{i\omega t} f(z,t) \tag{2}$$

exists. We further assume that $|\tilde{f}(z,\omega)|$ increases, at most, exponentially for large positive z, so that the Fourier-Laplace transform

$$F(k,\omega)=\int_0^{\infty} dz\, e^{-ikz}\tilde{f}(z,\omega) \tag{3}$$

exists for ω real and k in some suitable lower half-plane. If the frequency spread of the electromagnetic pulse is small in comparison with the center frequency (i.e., $\bar{\omega}\tau \gg 1$ in the notation below), we can solve Maxwell's equations in the form

$$[(\omega/c)n(\omega)-k]F(k,\omega)=S(\omega) \quad , \tag{4}$$

where

$$n(\omega)=n_\infty-\omega_0\omega_p/\omega(\omega-\omega_0+i\gamma), \quad |\omega_p/\gamma| \ll n_\infty, \tag{5}$$

is the refractive index of the medium, and $S(\omega)$ is a source field appropriate to the incident signal $(z=0^+)$.

Solving (4) for $F(k,\omega)$ and inverting the transform (3), we find

$$\tilde{f}(z,\omega)=iS(\omega)\exp[i(z\omega/c)n(\omega)] \tag{6}$$

for $z>0$. We choose the source field $S(\omega)$ such that, at $z=0^+$, $f(z,t)$ corresponds to an input pulse of mean frequency $(\bar{\omega}/2\pi)$ and amplitude $\exp(-t^2/2\tau^2)$:

$$iS(\omega)=\int_{-\infty}^{\infty} dt\, e^{i\omega t} e^{-i\bar{\omega}t} e^{-t^2/2\tau^2}$$

$$=\tau(2\pi)^{-1/2}\exp[-\tfrac{1}{2}(\omega-\bar{\omega})^2\tau^2] \quad . \tag{7}$$

Using this result with (6) and the inverse of (3), we obtain

$$f(z,t)=\tau/(2\pi)^{1/2}\int_{-\infty}^{\infty} d\omega\, e^{-i\omega t} \times e^{i\omega z n(\omega)/c} e^{-\frac{1}{2}(\omega-\bar{\omega})^2\tau^2} \tag{8}$$

for $z>0$ and t arbitrary. This equation is the starting point for the analytical and numerical exploration which occupies us for the rest of the paper. It describes the propagation of a plane wavefront, initially Gaussian pulse in a linear medium with refractive index (5).

In the description in Sec. I of a realistic experiment, we referred to the incidence of a Gaussian pulse on a slab containing the anomalous dispersion medium, whereas our function $f(z,t)$ refers to the field inside a semi-infinite block of material. The interior and exterior fields at frequency $\omega/2\pi$ differ by a factor which is an algebraic function of the refractive index $n(\omega)$. If $|\omega_p/\gamma| \ll 1$, as we assume, this factor is nearly constant in frequency and its inclusion would not significantly affect the qualitative results. It is of course true that geometric resonances similar to those familiar for Fabry-Perot cavities must be taken into account where they are important in laboratory measurements, but these are complications which have nothing directly to do with the topic of this paper and are ignored.

The source function $S(\omega)$ in (6) has been so chosen in (7) that an observer at $z=0$ measures a Gaussian pulse envelope which has a maximum value at $t=0$. We show in Secs. III and IV that in certain circumstances an observer at some position $z>0$ will measure a Gaussian pulse envelope of approximately the same temporal width as the input pulse but with its maximum value at some *previous* time $t<0$. This is *not* a violation of causality, but is instead a consequence of pulse-shape distortion. Although its amplitude is small for $|t|$ large, the Gaussian pulse

$$f(0,t)=e^{-i\bar{\omega}t} e^{-t^2/2\tau^2} \tag{9}$$

really has no true beginning or end. The $t<0$ envelope maximum seen by an observer at $z>0$ is not a direct reflection of the maximum of the input-pulse envelope, but arises from the action of the dispersive medium on the weak early components of that envelope. In this sense the group velocity described below is a specific attribute of a Gaussian pulse or, more generally, of any pulse which is approximately Gaussian near its maximum.

III. APPROXIMATIONS FOR $\gamma\tau \gg 1$ AND z SMALL

In this section, we consider the case for which the spectral width of the pulse is substantially less than the atomic linewidth, that is $\gamma\tau \gg 1$. Under these circumstances the principal contribution to the integral (8) comes from (circular)

frequencies ω in the neighborhood of the central frequency $\bar{\omega}$ of the input pulse, and we may approximate $\omega n(\omega)$ by the first few terms of the Taylor series

$$\omega n(\omega) = \bar{\omega} n(\bar{\omega}) + (\omega - \bar{\omega}) \left. \frac{d(\omega n)}{d\omega} \right|_{\bar{\omega}} + \tfrac{1}{2}(\omega - \bar{\omega})^2 \left. \frac{d^2(\omega n)}{d\omega^2} \right|_{\bar{\omega}} + \cdots , \tag{10}$$

where, from (5),

$$\frac{1}{m!} \left. \frac{d^m(\omega n)}{d\omega^m} \right|_{\bar{\omega}} = \frac{(-1)^m \omega_p \omega_0}{(\bar{\omega} - \omega_0 + i\gamma)^{m+1}} , \quad m \geq 2. \tag{11}$$

The series (10) diverges if $(\omega - \bar{\omega})^2 > [(\bar{\omega} - \omega_0)^2 + \gamma^2]$, so that this expansion is only useful when the important frequencies of (8) are those for which $(\omega - \bar{\omega})^2 \ll [(\bar{\omega} - \omega_0)^2 + \gamma^2]$. If $z > 0$ is sufficiently small, the important frequencies are those for which $(\omega - \bar{\omega})^2 \tau^2 \lesssim 1$, and, with $\gamma\tau \gg 1$, the Taylor series (10) converges rapidly. For $|\omega - \bar{\omega}|\tau = 1$, successive terms in (10) are smaller in magnitude by a factor $[(\bar{\omega} - \omega_0)^2 + \gamma^2]^{-1/2} \leq 1/\gamma\tau \ll 1$. For larger z, the divergence of (10) for $|\omega - \bar{\omega}|$ large can cause trouble; we return to this point later.

Assuming that the series (10) converges sufficiently rapidly, we truncate the series after three terms and substitute into (8) to obtain, with $u \equiv \omega - \bar{\omega}$,

$$f(z,t) = \frac{\tau}{2\pi} \exp\left[-i\omega\left(t - \frac{zn(\bar{\omega})}{c}\right)\right] \times \int_{-\infty}^{\infty} du \exp\left[-itu - \frac{u^2\tau^2}{2} + \frac{iz}{c}\left(u \left. \frac{d(\omega n)}{d\omega} \right|_{\bar{\omega}} + \frac{1}{2} u^2 \left. \frac{d^2(\omega n)}{d\omega^2} \right|_{\bar{\omega}}\right)\right] . \tag{12}$$

As long as

$$\mathrm{Re}\left(1 - \frac{iz}{c\tau^2} \left. \frac{d^2(\omega n)}{d\omega^2} \right|_{\bar{\omega}}\right) > 0 , \tag{13}$$

the integral (12) converges, to give

$$f(z,t) = \left(1 - \frac{iz}{c\tau^2} \left. \frac{d^2(\omega n)}{d\omega^2} \right|_{\bar{\omega}}\right)^{-1/2} \times \exp\left[-i\bar{\omega}\left(t - \frac{zn(\bar{\omega})}{c}\right)\right] \times \exp\left\{-\left(t - \frac{z}{c} \left. \frac{d(\omega n)}{d\omega} \right|_{\bar{\omega}}\right)^2 \times \left[2\tau^2\left(1 - \frac{iz}{c\tau^2} \left. \frac{d^2(\omega n)}{d\omega^2} \right|_{\bar{\omega}}\right)\right]^{-1}\right\} . \tag{14}$$

The inequality (13) will always obtain if z is small enough, but it does not generally obtain for z large. The term $(z/c\tau^2)[d^2(\omega n)/d\omega^2]_{\bar{\omega}}$ is of order $z\omega_0\omega_p/c\tau^2\gamma^3$, and, when this quantity is comparable to unity, the procedure of terminating the series (10), as we did in (12), becomes increasingly dubious. We return to this point later but, for the moment, take the view that $|z\omega_0\omega_p/c\tau^2\gamma^3| \ll 1$ and that the algebraic prefactor in (14) does not deviate significantly from unity, especially in comparison with variations in the remaining exponential factors.

We now proceed to an examination of those exponential factors. It is useful to separate $n(\omega)$ into its real and imaginary parts and to introduce new notation. Set

$$x = z\omega_0\omega_p/c\tau^2\gamma^3 , \tag{15}$$

$$\Gamma = \gamma\tau/\sqrt{2} , \tag{16}$$

$$T = \sqrt{2}\,(t - n_\infty z/c)/\tau , \tag{17}$$

$$\xi = (\bar{\omega} - \omega_0)/\gamma , \tag{18}$$

$$\kappa(\xi) = 1/(1 + \xi^2) , \tag{19}$$

$$\nu(\xi) = -\xi/(1 + \xi^2) . \tag{20}$$

Here x is the dimensionless distance variable which we have assumed small in comparison with unity. Γ is the ratio of the atomic to the pulse linewidth, which we are supposing in this section to be such that Γ is large compared to unity. T is a reduced time, giving, in units of the pulse width $\tau/\sqrt{2}$, the interval between some instant and the instant ($T=0$) at which the pulse peak would have arrived in the absence of anomalous dispersion. The quantities $\kappa(\xi)$ and $\nu(\xi)$ give, in dimensionless form, the absorptive and dispersive part of the refractive index in terms of the dimensionless frequency variable ξ.

Neglecting the algebraic prefactor, we can rewrite (14) in the form

$$f(z,t) = e^{i\bar{\omega}(t - zn_\infty/c)} e^{\Delta_1(T,x) + i\Delta_2(T,x)} , \tag{21}$$

where one can show after a good deal of algebra that

$$\Delta_1(T,x) = -2\Gamma^2 x\left(\kappa - \frac{\frac{1}{2}(\kappa')^2 x}{1+\kappa'' x}\right) - \frac{\frac{1}{4}(1+\kappa'' x)}{(1+\kappa'' x)^2+(\nu'' x)^2} \times \left[T - 2\Gamma x\left(\nu' - \frac{\nu''\kappa' x}{1+\kappa'' x}\right)\right]^2 , \quad (22)$$

$$\Delta_2(T,x) = 2\Gamma^2 x\left(\nu + \frac{(\kappa')^2}{2\nu''}\right) + \frac{\frac{1}{4}\nu'' x}{(1+\kappa'' x)^2+(\nu'' x)^2} \times \left(T - \frac{2\Gamma}{\nu''}\left[\kappa' + (\kappa'\kappa'' + \nu'\nu'')x\right]\right)^2 . \quad (23)$$

Look first at the expression (22), which governs the amplitude of the pulse (21). If we sit at a fixed x and examine the temporal change in the pulse amplitude, we still find a pulse of Gaussian shape whose width is not appreciably different from that of the incident pulse until x becomes of order unity. The peak of the Gaussian pulse initially varies as $\exp(-2\Gamma^2\kappa x)$, with departure from this simple exponential behavior only when x becomes of order unity. At any given x, the instant corresponding to the peak of the pulse in units of the reduced time is

$$T_1 = 2\Gamma x\left(\nu' + \frac{\nu''\kappa' x}{1+\kappa'' x}\right), \quad (24)$$

of which the first term is just what would be given for $|\omega_p/\gamma| \ll 1$ by the classical group velocity $c/[n_r(\bar{\omega}) + \bar{\omega} dn_r/d\omega]$, where $n_r(\omega) = \mathrm{Re}[n(\omega)]$.

This is quite a paradoxical result. Consider, for example, an absorbing medium, for which $\omega_p > 0$, with the pulse center frequency $\bar{\omega}$ and atomic line center ω_0 coincident ($\xi = 0$). Then we have $c/[n_r(\bar{\omega}) + \bar{\omega} dn_r/d\omega] = c/[n_\infty - \omega_0\omega_p/\gamma^2]$. We have required that $\omega_p \ll \gamma$, but not that $\omega_0\omega_p < \gamma^2$, so the denominator can have either sign. So, not only can the pulse appear to travel (in the sense of tracing the locus of instants of maximum amplitude) faster than c: it can even appear to travel backwards. A similar situation exists for an inverted medium ($\omega_p < 0$), not at the center of the line but in the wings ($|\xi| > 1$). The nervous reader may perhaps feel reassured if we point out (i) that, in any time snapshot, the amplitude decreases monotonically with z in a lossy medium, and (ii) that the Poynting vector is always directed toward increasing z. Nevertheless, it is still true that the output-pulse peak can sometimes emerge from the far side of a parallel-sided slab of medium *before* the peak of the input pulse enters the near side. This output pulse will be greatly attenuated (or greatly amplified, as the case may be) but still of substantially the same Gaussian shape as the input pulse.

These statements follow from Eqs. (21) and (22) and are accurate as long as $|x| \ll 1$. That is, the slab must be thinner than something like $\gamma^2\tau^2$ exponential-decay (or growth) lengths, a condition that is not really very restrictive so long as the pulse is spectrally very much narrower than the atomic line ($\gamma\tau \gg 1$). The paradoxical statements do *not* violate causality, but reflect, as we mentioned in Sec. II, pulse-shape distortion even though the pulse does not appear to be distorted! The output pulse which leaves before the entrance of the peak of the input pulse is formed from field components in the leading edge of the input pulse and not, to any substantial degree, from components at the input-pulse peak.

Consider next the phase function $\Delta_2(T,x)$ of Eq. (23). At any given x, this shows a quadratic time variation of phase, which implies a modulation of the frequency of the pulse. If we write

$$\Delta_2(T,x) = A_1(x) + [T - T_2(x)]^2 A_2(x), \quad (25)$$

then the frequency shift $\delta\Omega(x)$ (in units of $\sqrt{2}/\tau$) at the instant $T_1(x)$ of maximum amplitude is

$$\delta\Omega = \left.\frac{\partial\Delta_2}{\partial T}\right|_{T_1} = 2(T_1 - T_2)A_2. \quad (26)$$

Substitution from Eqs. (23) and (24) yields the result

$$\delta\Omega(x) = -\Gamma\kappa' x/(1+\kappa'' x). \quad (27)$$

Inspection shows that the sense of the shift is as follows. When the medium is absorbing, a pulse with $\xi \neq 0$ (i.e., $\bar{\omega} \neq \omega_0$) is shifted in frequency away from the center of the line; when the medium is amplifying, it is shifted towards the center. The magnitude of the shift is such that, when x is of order unity, the shift is of the order of the atomic linewidth. Physically the frequency shift results because in an absorbing medium, for example, those Fourier components of the pulse that lie nearer line-center are attenuated more than those in the wings; consequently, the center of gravity of the spectrum of the pulse shifts away from line-center.

The expression (25) also predicts a certain amount of "chirping" in the transmitted pulse. Write (25) in the form

$$\Delta_2(T,x) = [A_1 + (T_1 - T_2)^2 A_2] + 2(T - T_1)(T_1 - T_2)A_2 + (T - T_1)^2 A_1. \quad (28)$$

The first term is time-independent, the second represents the frequency shift already discussed, and the third describes the chirping. This third term is zero at the instant the pulse amplitude is greatest ($T = T_1$), and it increases in magnitude with temporal separation from T_1 in either direction. For the chirping to be qualitatively significant, we require that this term have a magnitude substan-

tially larger than unity before $(T - T_1)$ is such that the pulse no longer has appreciable amplitude. It follows from Eqs. (21) – (25) that at the $1/e$ point we have

$$(T - T_1)^2 A_2 = \nu'' x/(1 + \kappa'' x) \quad , \tag{29}$$

which is always less than order unity for those x within the range of validity of the analysis, so that chirping is not in fact very substantial.

These various results derive from the approximation (21) to the exact result (8). They accurately describe the propagation of a Gaussian pulse as long as $z > 0$ is small enough that $|x| \ll 1$. The approximation (21) is based upon the truncated-power-series approximation (12) and is only valid as long as that approximation is accurate. [The algebraic prefactor omitted in going from (14) to (21) is really not very important even if $|x| \gtrsim 1$.] It may be shown that a necessary and sufficient condition is

$$|x| \ll \sqrt{2}\Gamma(1 + \xi^2)/(1 + \kappa'' x). \tag{30}$$

When this condition is met, the integral (12) converges [because (13) obtains] and the terms omitted from the exponent by the truncation are all much less in magnitude than unity over the important range of frequencies.

When the inequality (30) is violated, the quadratic truncation used in (12) is inadequate and more elaborate procedures are required. Because the power series (10) has a finite radius of convergence, it is *not* generally sufficient (or useful) to improve (12) by including a few more terms of the series. It is necessary to approximate $\omega n(\omega)$ accurately over a broad range of frequencies, for some of which $(\omega - \bar{\omega})^2 > [(\bar{\omega} - \omega_0)^2 + \gamma^2]$. In this regard it is important to note that the difficulties in (12) for x large arise solely from the truncated-power-series approximation and are not intrinsic to the exact integral (8); that integral is mathematically well behaved for all finite x.

Information as to which frequencies are important in (8) is contained in the pulse power spectrum

$$P(z, \omega) = |\tilde{f}(z, \omega)|^2$$

$$= 2\pi\tau^2 \exp[-(\omega - \bar{\omega})^2 \tau^2 - (2z\omega/c)\mathrm{Im}n(\omega)]$$

$$= 2\pi\tau^2 \exp\left(-(\omega - \bar{\omega})^2 \tau^2 - \frac{2z\omega_0 \omega_p \gamma/c}{(\omega - \omega_0)^2 + \gamma^2}\right). \tag{31}$$

In the notation of Eqs. (15) – (20), the approximations used in (12) give

$$P(z, \omega) = 2\pi\tau^2 \exp\{-4\Gamma^2 \kappa x - 4\Gamma^2 \kappa' x[(\omega - \bar{\omega})/\gamma]$$

$$- 2\Gamma^2(1 + \kappa'' x)[(\omega - \bar{\omega})/\gamma]^2\} \ , \tag{32a}$$

$$P(z, \omega) = 2\pi\tau^2 \exp -\left[4\Gamma^2 x\left(\kappa - \frac{\frac{1}{2}(\kappa')^2 x}{1 + \kappa'' x}\right)\right.$$

$$\left. - 2\Gamma^2(1 + \kappa'' x)[(\omega - \bar{\omega}_x)/\gamma]^2\right], \tag{32b}$$

where $\bar{\omega}_x = \bar{\omega} - \gamma\kappa' x/(1 + \kappa'' x)$. (33)

This is a Gaussian power spectrum with an over-all amplitude consistent with the first (T-independent) term of (22) and with a center frequency $\bar{\omega}_x$ consistent with (27). The width of the Gaussian (32) is larger, however, than what one would deduce from the second T-dependent or amplitude-modulation term of (22). This extra width derives from the frequency modulation implicit in the T dependence of (23).

We have not been able to find simple useful analytic approximations to $f(z, t)$ which are valid for $|x| \gtrsim 1$. We have, however, evaluated $f(z, t)$ numerically for a range of parameters (x, Γ, ξ). Those results are discussed in Sec. IV below. For $|x|$ small, they coincide with that we would predict from (21) and (32). As the inequality (30) becomes less strong, deviations become more significant. If $\Gamma \equiv \gamma\tau/\sqrt{2} \gg 1$, such deviations set in for values of $|\Gamma^2 x|$ which are so large that the over-all gain or attenuation implicit in the first term of (22) would be enormous – so large, in fact, that the effects would be very difficult to observe in the laboratory with pulses weak enough to justify our initial assumption of linear response. In this sense the results for $|x| \gtrsim 1$ are largely only of academic interest and the approximate expressions (21) – (23) and (32) the important results.

IV. NUMERICAL RESULTS

In. Sec. III, we described approximations to $f(z, t)$ useful when $\Gamma \equiv \gamma\tau/\sqrt{2} \gg 1$ and $|x| \equiv |z\omega_p \omega_0/c\tau^2\gamma^3|$ not too large. In order to explore how those approximations fail as $|x|$ increases, we also evaluated the integral in (8) numerically for a range of parameters (x, Γ, ξ). Those results are described herein.

All of the results reported correspond to $\Gamma \equiv \gamma\tau/\sqrt{2} = 4$. For smaller Γ, the approximations of Sec. III fail too soon to be of much interest. For larger Γ, perhaps the case of greatest interest with pulsed laser laboratory sources, those approximations fail only for $|\Gamma^2 x|$ so large that the gain or attenuation factor implicit in the first term of (22) makes the calculation irrelevant. The choice $\Gamma = 4$ is intermediate between these extremes and convenient to accommodate on the computer.

The power spectrum (31) is plotted versus fre-

quency difference $\Delta\Omega(\omega) \equiv (\omega - \bar{\omega})\tau/\sqrt{2}$ for $\xi \equiv -\Delta\Omega(\omega_0)/\Gamma = 0$, 0.25, 0.5, 1.0, and 2.0 in Figs. 1–5, respectively. The different (solid) curves in each figure correspond to different values of $x \equiv z\omega_p\omega_0/c\tau^2\gamma^3$. The case $x > 0$ corresponds to attenuation, $x < 0$ to gain, and $x = 0$ to the undistorted input spectrum. The two dashed curves in each figure trace out the loci of the spectral maxima appropriate to the exact spectrum (31) and to the Gaussian approximation (32). A Gaussian power spectrum corresponds to a parabola in the semilog plots of Figs. 1–5. The extent to which a particular curve deviates from a parabola near its maximum and the degree to which the two dashed-line loci diverge are two measures of the accuracy of the power-series truncation procedure described in Sec. III.

The pulse amplitude $|f(z,t)|$ seen at a particular point z is plotted as a function of the reduced time $T = (t - n_\infty z/c)\sqrt{2}/\tau$ for these same values of ξ in Figs. 6–10, respectively. In each case, only the neighborhood of the pulse maximum is shown. The edges of the pulse are generally not Gaussian, but their intensity is very much less than that of the pulse maximum. A Gaussian pulse corresponds to a parabola in the semilog plots of Figs. 6–10. Near the maximum the pulse is Gaussian, except for particular cases; for example, the $x > 0$ curves of Fig. 6, $\xi = 0$.

As in Figs. 1–5, the different (solid) curves in each figure correspond to different values of x.

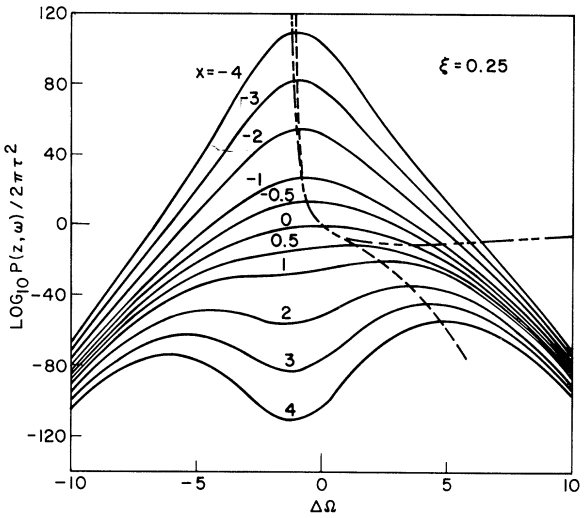

FIG. 2. Power spectra for system with $\Gamma \equiv \gamma\tau/\sqrt{2} = 4$ and $\xi \equiv (\bar{\omega} - \omega_0)/\gamma = 0.25$. The different solid curves are the spectra computed from Eq. (31) for different values of $x \equiv z\omega_p\omega_0/c\tau^2\gamma^3$ as a function of the frequency difference $\Delta\Omega \equiv (\omega - \bar{\omega})\tau/\sqrt{2}$. The dashed curves are the loci of the spectral maxima appropriate to the exact spectrum (shown) and to the Gaussian approximation (32).

The two dashed curves trace out the loci of the pulse maxima appropriate to the exact (numerical) and approximate (21) expressions. It is obvious

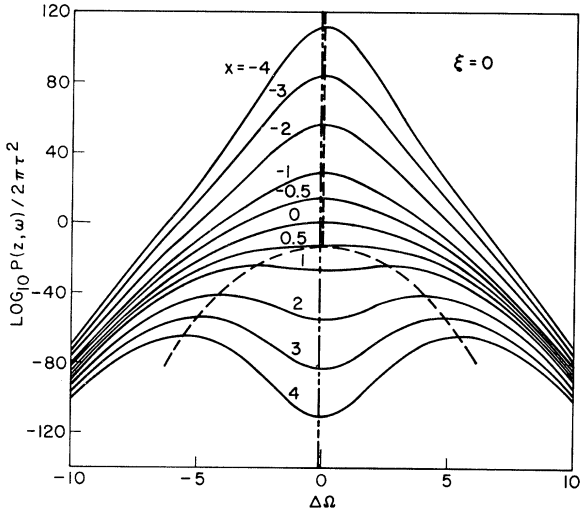

FIG. 1. Power spectra for system with $\Gamma \equiv \gamma\tau/\sqrt{2} = 4$ and $\xi \equiv (\bar{\omega} - \omega_0)/\gamma = 0$. The different solid curves are the spectra computed from Eq. (31) for different values of $x \equiv z\omega_p\omega_0/c\tau^2\gamma^3$ as a function of the frequency difference $\Delta\Omega \equiv (\omega - \bar{\omega})\tau/\sqrt{2}$. The dashed curves are the loci of the spectral maxima appropriate to the exact spectrum (shown) and to the Gaussian approximation (32).

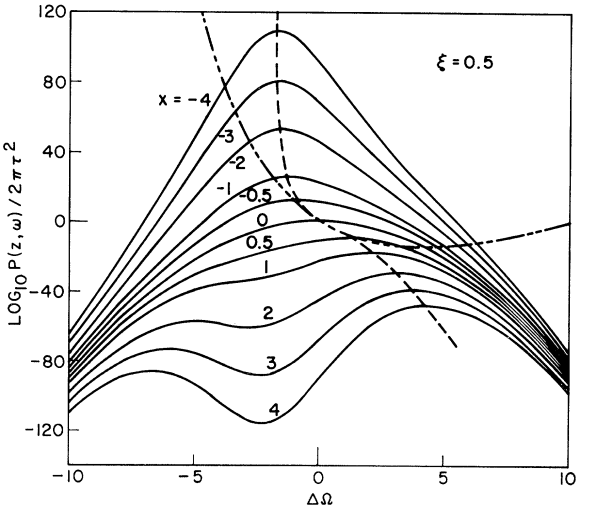

FIG. 3. Power spectra for system with $\Gamma \equiv \gamma\tau/\sqrt{2} = 4$ and $\xi \equiv (\bar{\omega} - \omega_0)/\gamma = 0.5$. The different solid curves are the spectra computed from Eq. (31) for different values of $x \equiv z\omega_p\omega_0/c\tau^2\gamma^3$ as a function of the frequency difference $\Delta\Omega \equiv (\omega - \bar{\omega})\tau/\sqrt{2}$. The dashed curves are the loci of the spectral maxima appropriate to the exact spectrum (shown) and to the Gaussian approximation (32).

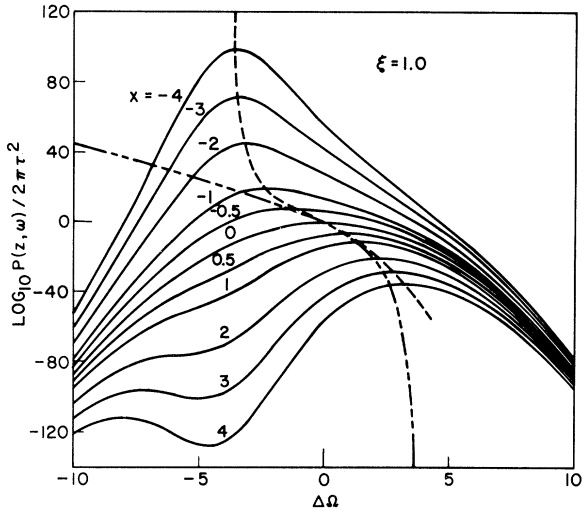

FIG. 4. Power spectra for system with $\Gamma \equiv \gamma\tau/\sqrt{2} = 4$ and $\xi \equiv (\bar{\omega} - \omega_0)/\gamma = 1.0$. The different solid curves are the spectra computed from Eq. (31) for different values of $x \equiv z\omega_p\omega_0/c\tau^2\gamma^3$ as a function of the frequency difference $\Delta\Omega \equiv (\omega - \bar{\omega})\tau/\sqrt{2}$. The dashed curves are the loci of the spectral maxima appropriate to the exact spectrum (shown) and to the Gaussian approximation (32).

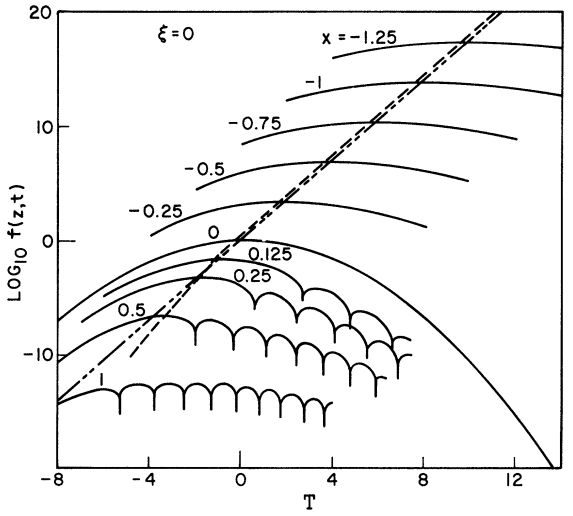

FIG. 6. Amplitude of pulse $f(z,t)$ seen at a particular space point z as a function of the reduced time $T = (t - n_\infty z/c)\sqrt{2}/\tau$ for system with $\Gamma = 4$ and $\xi = 0$. The different solid curves correspond to different values of $x \equiv z\omega_p\omega_0/c\tau^2\gamma^3$. The dashed curves are the loci of the peak maxima appropriate to the exact solution (shown) and to the approximation (21).

from the figures that the approximations of Sec. III are accurate for $|x|$ sufficiently small, but that they are inaccurate for larger $|x|$, especially those values which violate the inequality (30). It is also obvious from the power spectra of Figs. 1–5 why the approximations of Sec. III fail

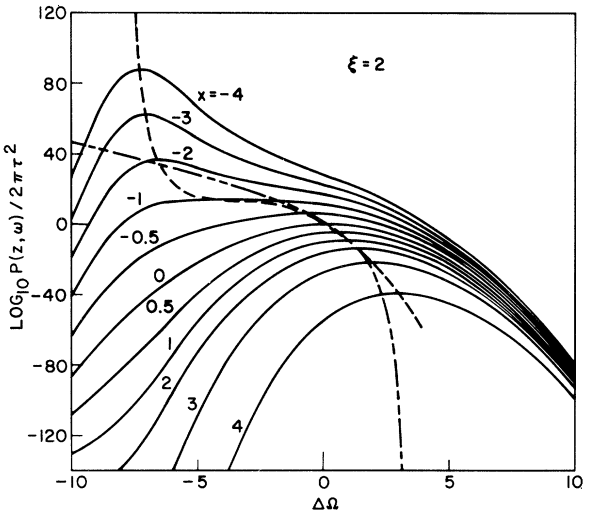

FIG. 5.. Power spectra for system with $\Gamma \equiv \gamma\tau/\sqrt{2} = 4$ and $\xi \equiv (\bar{\omega} - \omega_0)/\gamma = 2.0$. The different solid curves are the spectra computed from Eq. (31) for different values of $x \equiv z\omega_p\omega_0/c\tau^2\gamma^3$ as a function of the frequency difference $\Delta\Omega \equiv (\omega - \bar{\omega})\tau/\sqrt{2}$. The dashed curves are the loci of the spectral maxima appropriate to the exact spectrum (shown) and to the Gaussian approximation (32).

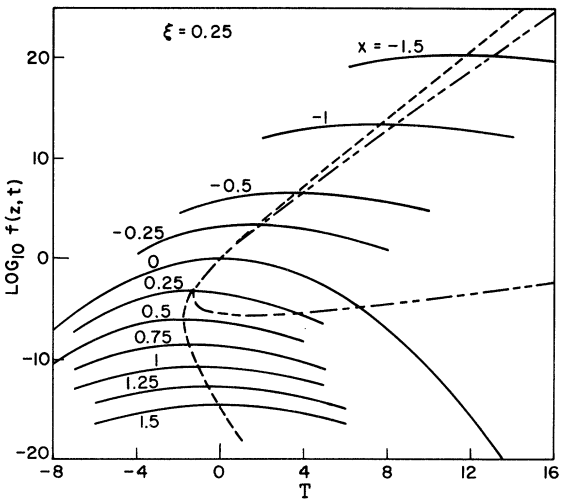

FIG. 7. Amplitude of pulse $f(z,t)$ seen at a particular space point z as a function of the reduced time $T = (t - n_\infty z/c)\sqrt{2}/\tau$ for system with $\Gamma = 4$ and $\xi = 0.25$. The different solid curves correspond to different values of $x \equiv z\omega_p w_0/c\tau^2\gamma^3$. The dashed curves are the loci of the peak maxima appropriate to the exact solution (shown) and to the approximation (21).

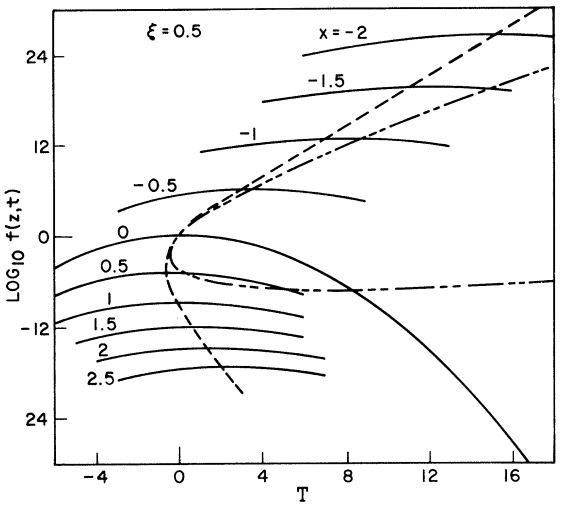

FIG. 8. Amplitude of pulse $f(z,t)$ seen at a particular space point z as a function of the reduced time $T=(t-n_\infty z/c)\sqrt{2}/\tau$ for system with $\Gamma=4$ and $\xi=0.5$. The different solid curves correspond to different values of $x\equiv z\omega_p\omega_0/c\tau^2\gamma^3$. The dashed curves are the loci of the peak maxima appropriate to the exact solution (shown) and to the approximation (21).

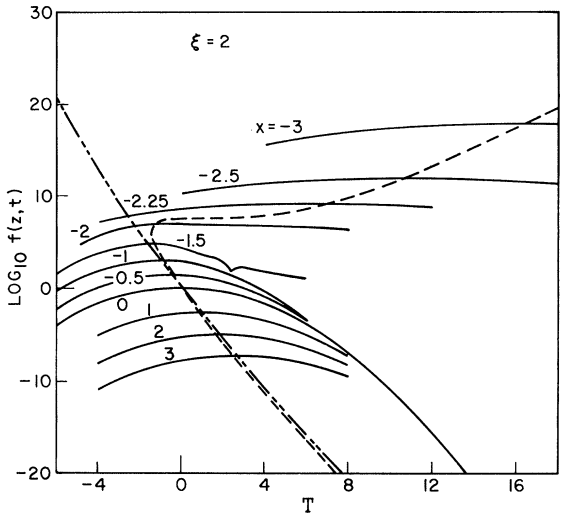

FIG. 10. Amplitude of pulse $f(z,t)$ seen at a particular space point z as a function of the reduced time $T=(t-n_\infty z/c)\sqrt{2}/\tau$ for system with $\Gamma=4$ and $\xi=2.0$. The different solid curves correspond to different values of $x\equiv z\omega_p\omega_0/c\tau^2\gamma^3$. The dashed curves are the loci of the peak maxima appropriate to the exact solution (shown) and to the approximation (21).

where they do. In Eq. (12) and those following it, we, in effect, approximate these rather complex power spectra by the first few terms of a power-series expansion about $\Delta\Omega=0$, where $\Delta\Omega(\omega)\equiv(\omega-\bar{\omega})\tau/\sqrt{2}$. The most important spectral range is that near where the power spectrum is greatest, and our approximations are accurate only so long as that maximum is nearly parabolic in shape and occurs near $\Delta\Omega=0$.

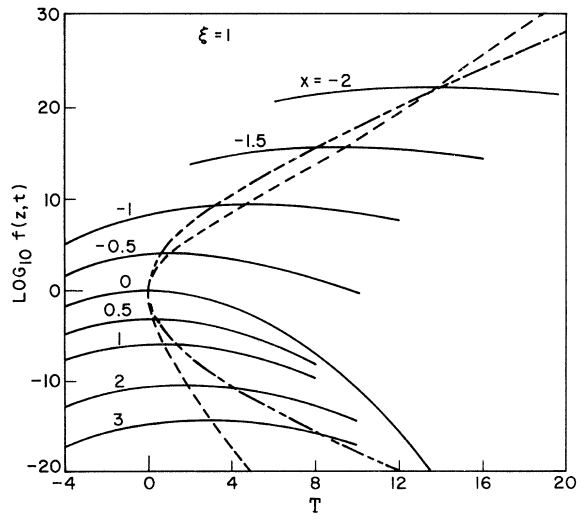

FIG. 9. Amplitude of pulse $f(z,t)$ seen at a particular space point z as a function of the reduced time $T=(t-n_\infty z/c)\sqrt{2}/\tau$ for system with $\Gamma=4$ and $\xi=1.0$. The different solid curves correspond to different values of $x\equiv z\omega_p\omega_0/c\tau^2\gamma^3$. The dashed curves are the loci of the peak maxima appropriate to the exact solution (shown) and to the approximation (21).

Consider as a specific example the case $\xi=0.5$ illustrated in Figs. 3 and 8. Near its maximum, each power spectrum shown in Fig. 3 is approximately Gaussian and, as we might therefore expect, each pulse in Fig. 5 is also approximately Gaussian (near its peak). However, the position of the power-spectrum maximum shifts away from $\Delta\Omega=0$ at $x=0$ to $\Delta\Omega=-2$ at $x=-\infty$ and to large positive values for $x\to+\infty$; the spectrum is not accurately Gaussian from these displaced maxima to $\Delta\Omega=0$; and the approximations of Sec. III fail, as indicated by the divergence of the dashed curves. Analytic approximations valid for general x could be based upon power-series expansions about the power-spectrum maximum (rather than about the incident-pulse center frequency $\bar{\omega}$), but the resulting expressions would be considerably more complex than those of Sec. III.

Such a more general approximation technique would also fail if the spectrum was definitely not Gaussian near its maximum; that is, if a quadratic approximation in the exponent was inadequate. For these cases the output-pulse amplitude would generally not be Gaussian, even near its maximum. Cases illustrating this pathology occur in our examples, especially those for $\xi=0$, $x>0$, and $\xi=2$,

$-2.5 < x < -1$. Fortunately, most cases are not of this type; none are for $|x|$ sufficiently small.

The case $\xi = 0$, $x > 0$, is sufficiently curious to warrant further discussion. For $x < 0$, the medium is amplifying, the power spectrum (Fig. 1) sharpens but remains approximately Gaussian near its maximum at $\Delta\Omega = 0$, and the pulse amplitude (Fig. 6) remains Gaussian, except in the relatively weak leading and trailing edges. Because the spectral maximum remains at $\Delta\Omega = 0$ for $x \lesssim 0$, we expect the approximations of Sec. III to be particularly good for negative x. The situation is very different for $x > 0$, although for $x \approx 0$ the approximations of Sec. III are still accurate near the peak of the output-pulse amplitude. As x increases further, the quadratic approximation used in (12) and thereafter deteriorates until for $x \gtrsim 0.5$ the criterion (13) fails. By this point, however, the output-pulse amplitude exhibits a sinusoidalike oscillation extending for $x \gtrsim 0.75$ right through the peak. These curious oscillations are peculiar to $\xi \approx 0$ and are not observed in the $\xi \geq 0.25$ examples of Figs. 7–10. Vestiges are apparent, however, at $\xi = 0.05$ as shown in Fig. 11.

One is tempted by the apparent simplicity of (8) for $\omega_0 = \bar{\omega}$ to search for an analytic approximation which will describe the oscillations seen in Figs. 6 and 11. We have wasted a great deal of time on such a search without significant success. We have shown that qualitatively similar oscillations occur if the input spectrum is Lorentzian rather than Gaussian, but even in this case no simple but general closed-form expressions have been found. The problem remains an unmet challenge.

Although the approximations of Sec. III do generally break down for $|x|$ large, the numerical results confirm their validity for $x \approx 0$, the case of greatest importance in pulsed laser laboratory studies. The calculations also confirm that the concept of group velocity has meaning for an absorptive medium. Broadly speaking, a Gaussian input pulse remains Gaussian, and the peak of the pulse moves in space with an apparent velocity related to the classical group-velocity expression, even if that velocity is greater than the velocity of light in vacuum or is negative. For thick slabs ($|x| \gtrsim 1$), the temporal width and the spectral composition of the pulse generally will be different from that of the input pulse. The numerical results for $|x|$ large can be understood in the context of Sec. III if we view a thick slab as a composite of many thin slabs into each of which a Gaussian pulse is injected (from the slab before) and to which the equations of Sec. III pertain, with a suitably varying pulse width τ and central frequency $\bar{\omega}$. However, even this technique will fail for $\xi = 0$, $x > 0$, because there the concept of a dominant central frequency $\bar{\omega}$ eventually fails.

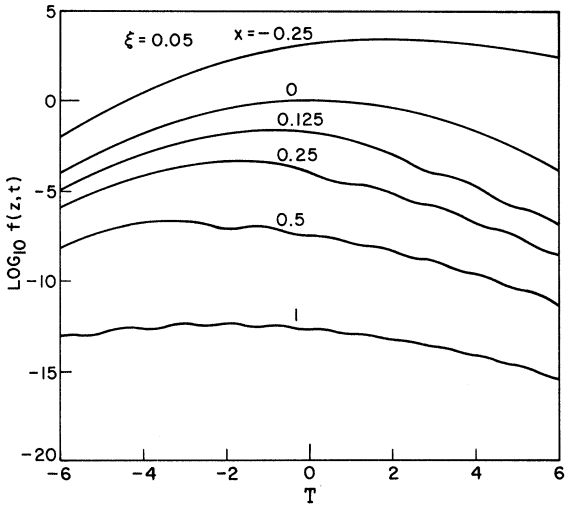

FIG. 11. Amplitude of pulse $f(z,t)$ seen at a particular space point z as a function of the reduced time $T = (t - n_\infty z/c)\sqrt{2}/\tau$ for system with $\Gamma = 4$ and $\xi = 0.05$. The different solid curves correspond to different values of $x \equiv z\omega_p\omega_0/c\tau^2\gamma^3$.

---

[1]A. Sommerfeld, Z. Physik 8, 841 (1907).

[2]English translations of the important Sommerfeld-Brillouin papers are contained in L. Brillouin, Wave Propagation and Group Velocity (Academic Press Inc., New York, 1960).

[3]L. Brillouin, Ann. Physik 44, 203 (1914).

[4]P. Pleshko and I. Palócz, Phys. Rev. Letters 22, 1201 (1969).